Recenzované výzkumné články

Effect of Cooling of the Ingot on its Macro-structural and Chemical Heterogeneity

Vliv intenzivního chlazení ingotu na jeho makrostrukturní a chemickou heterogenitu

Ing. Jaroslav Pindor, Ph.D.[1]; **Ing. Vladislav Kurka, Ph.D.**[1]; **Ing. Jana Kosňovská**[1]; **Ing. Šárka Štefanišinová**[1]; **doc. Ing. Ladislav Socha, Ph.D.**[2]; **prof. Dr. Ing. René Pyszko**[3]

[1] MATERIÁLOVÝ A METALURGICKÝ VÝZKUM s.r.o., Pohraniční 693/31, 703 00 Ostrava-Vítkovice, the Czech Republic

[2] VŠB – Technical University of Ostrava, Faculty of Metallurgy and Materials Engineering, Department of Metallurgy and Foundry, 17. listopadu 15/2172, 708 33 Ostrava-Poruba, the Czech Republic

[3] VŠB – Technical University of Ostrava, Faculty of Metallurgy and Materials Engineering, Department of Thermal Engineering, 17. listopadu 15/2172, 708 33 Ostrava-Poruba, the Czech Republic

The company MATERIÁLOVÝ A METALURGICKÝ VÝZKUM s.r.o. (Material and Metallurgical Research, Ltd.) deals with the research project entitled "Technology of Intensive Cooling of Steel Cast into an Ingot Mould." This project is funded by the programme "Support of Science and Research in the Moravian-Silesian Region 2015." As part of the project, the technology of intensive cooling of steel cast into moulds has been tested. The project solution was divided into two parts. Two ingots of the same type were cast, where the cast steel was of the identical chemical composition, temperature and casting speed. In both cast ingots, the macro-structural and chemical heterogeneity of cast steel was compared in four zones in one longitudinal axial section and three transverse sections along the height of the ingot. The evaluated macrostructures in the ingot sections show that the effect of intense cooling of cast ingot has significantly manifested itself at the bottom of the ingot with the increased zone of coarse-grained, differently oriented crystals. The analysis of the macro-structure of the cooled and non-cooled ingot further shows that in the bottom part of the cooled ingot the porosity has increased, and on the contrary, the upper part of the ingot has shown a significantly reduced porosity. Another finding is that the intense heat transfer during the ingot casting and solidification has a major effect on reducing the segregation of C, Cr and Mo elements. The calculation of the heat score shows that approximately 20 % of the heat was removed from the cooled ingot compared to the non-cooled ingot. The highest increase in heat output was identified at the bottom of the ingot.

Keywords: *steel, ingot; steel cooling; ingot casting; chemical homogeneity; macro-structural homogeneity, heat transfer*

Společnost MATERIÁLOVÝ A METALURGICKÝ VÝZKUM s.r.o. řeší výzkumný projekt „Technologie intenzivního chlazení oceli odlité do kokily“ Tento projekt je podpořen z programu „Podpora vědy a výzkumu v Moravskoslezském kraji 2015“ V rámci projektu byla odzkoušena technologie intenzivního chlazení oceli odlité do kokil. Řešení projektu bylo rozděleno na 2 části. Byly odlity dva ingoty stejného typu. Odlitá ocel měla v obou případech stejné chemické složení, stejnou teplotu a rychlost odlévání. U obou ingotů byla porovnána makrostrukturní a chemická heterogenita odlité oceli ve čtyřech zónách v podélném osovém řezu a třech příčných řezech po výšce ingotu. Hodnocené makrostruktury v řezech ingotů prokazují, že vliv intenzivního chlazení odlévaného ingotu se projevil velmi výrazně v patní části ingotu, kde došlo ke zvětšení zóny hrubých, různě orientovaných krystalů. Z provedeného rozboru makrostruktury chlazeného a nechlazeného ingotu dále vyplývá, že ve spodní části chlazeného ingotu došlo ke zvětšení výskytu pórovitosti a naopak v horní části ingotu došlo k jejímu výraznému zmenšení. Dále bylo zjištěno, že intenzivní odvod tepla během odlévání a během tuhnutí ingotu má zásadní vliv na snížení odmíšení prvků C, Cr a Mo. Výpočet tepelné bilance prokázal, že z chlazeného ingotu bylo odvedeno o cca 20 % tepla více než u nechlazeného ingotu. Nejvyšší nárůst odvedeného tepla byl zjištěn ve spodní části ingotu.

Klíčová slova: *ocel; ingot; chlazení oceli; lití ingotu; chemická homogenita; makrostrukturní homogenita; přenos tepla*

The technology of intensive steel cooling during casting of ingots was tested as part of the project "Technology of Intensive Cooling of Steel Cast into an Ingot Mould", that is the subject of the company MATERIÁLOVÝ A

Hutnické listy č. 3/2017, roč. LXX
ISSN 0018-8069

METALURGICKÝ VÝZKUM s.r.o. (Material and Metallurgical Research, Ltd.). The project solution was divided into two parts. Two ingots of the same type were cast, where the cast steel was of the identical chemical composition, and in both instances the temperature and casting speed conditions were met. In both cast ingots, the macro-structural and chemical heterogeneity of cast steel in one longitudinal axial section and three transverse sections along the height of the ingot was compared. We compared the heat output through the mould wall and set the amount of heat transfer from the cooling.

1. Characteristics of pilot experiments

For the experiments, i.e. casting of a reference ingot (Experiment Part 1) and subsequent comparison with the ingot that was tested for the intensive cooling technology (Experiment Part 2), we selected the steel grade ČSN 14209 modified with molybdenum. In this publication, this steel is also referred to as 14209Mo. The required chemical composition of 14209Mo steel and the chemical composition of the cast melt from an induction furnace (hereinafter referred to as IF) into a casting ladle (hereinafter referred to as CL) are listed in Tab. 1.

Tab. 1 Required and target chemical composition of the steel grade 14209Mo
Tab. 1 Požadované a cílové chemické složení značky oceli 14209Mo

14209Mo Steel		Chemical composition (wt. %)										$T_{liq.}$ (°C)
		C	Si	Mn	Cr	Mo	Cu	Ni	P	S	Al	
Requirement	Min.	0.90	0.35	0.90	1.30	1.20	-	-	-	-	-	1471
	Max.	1.10	0.65	1.20	1.65	1.30	0.250	0.30	0.027	0.030	0.010	1450
Melt in CL Experiment, Part 1		1.00	0.44	0.99	1.53	1.24	0.035	0.08	0.018	0.009	0.018	1457
Melt in CL Experiment, Part 2		1.01	0.52	1.03	1.55	1.26	0.03	0.12	0.025	0.008	0.021	1458

The experiment progressed as follows. The melt was produced in an atmospheric IF. The mass of the melting was 1750 kg. After melting of the basic charge and alloying additives, the chemical composition was tested and element contents were adjusted to a desired range.

After heating to a casting temperature of 1598 °C, the melt was cast into a CL. By pouring it into the CL the melt was cooled to 1551 °C. The relatively high casting temperature, 94 °C above the liquids temperature, was chosen on the basis of long-term practical experience with casting these types of steels because the liquid steel in the low-capacity ladle cools faster. The melt produced in IF was poured to CL, where the sampling of the metal for chemical analysis was followed by the covering of the melt level with slag. The chemical composition of the melt (Experiment Part 1) in the ladle is shown in Table 1. Subsequently, the casting of a melt in a mould set started within approx. 1 min. The melt was poured under a protective argon atmosphere from the bottom into a V2A type-mould set. The casting time of a body of the ingot was 5.5 min. and the casting time of the whole ingot 7.2 min. In the Experiment Part 2, the technology of intensive cooling of cast steel was applied from the beginning of the mould filling. The weight of cast ingots was 1690 kg. After solidifying in a mould after approx. 60 minutes, the two ingots were stripped and placed in an annealing furnace for soft annealing at a temperature of 770 °C for 4 hours, followed by slow cooling in the furnace.

2. Evaluation of achieved results

Evaluation of the Experiment Part 1 was carried out in a published paper by the authors [1]. The ingots were transversely to the longitudinal axis cut into four samples on which the above parameters were examined in longitudinal axial sections I, II, III and IV. For these samples, the cast ingot macro-structure was evaluated. Samples were taken from cross-sections marked as cross-section A, B and C. In these samples, the chemical composition from the ingot edge to its centre was determined and its macro-structure also evaluated. The diagram of the ingot cutting with sampling points and their marking is shown in Fig. 1.

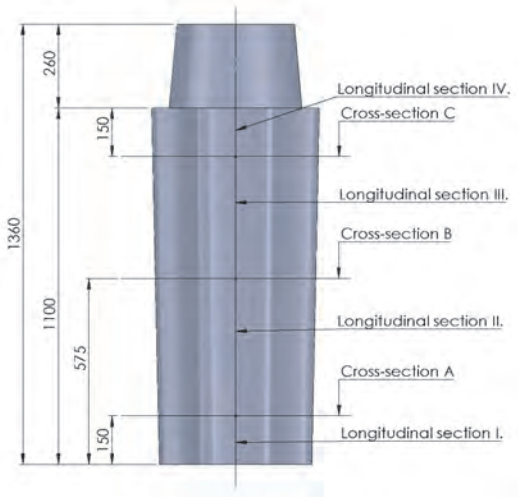

Fig. 1 Removing and marking of metal samples for evaluation in the longitudinal and transverse direction
Obr. 1 Odebrání a značení vzorků kovu k hodnocení jak v podélném, tak v příčném směru

2.1 The macrostructure evaluation

The evaluation of macrostructure was carried out using an accredited test QI-ISO-LAB4-40-01 "Macrostructure Testing with Etchings." The macrostructure of all examined samples was induced by etching in 10% HNO_3.

The actual macro-structural evaluation of the Experiment, Part 2, was carried out for each longitudinal section I through IV, followed by arranging these macro-structural analyses in sequence according to the location of individual sections of the longitudinal axis section of the ingot (Fig. 2). In addition, the macrostructures in cross-sections A, B and C were evaluated, which corresponded to the findings obtained in the longitudinal axis of the ingot. For illustration, these cross sections with macrostructure are shown in Fig. 3.

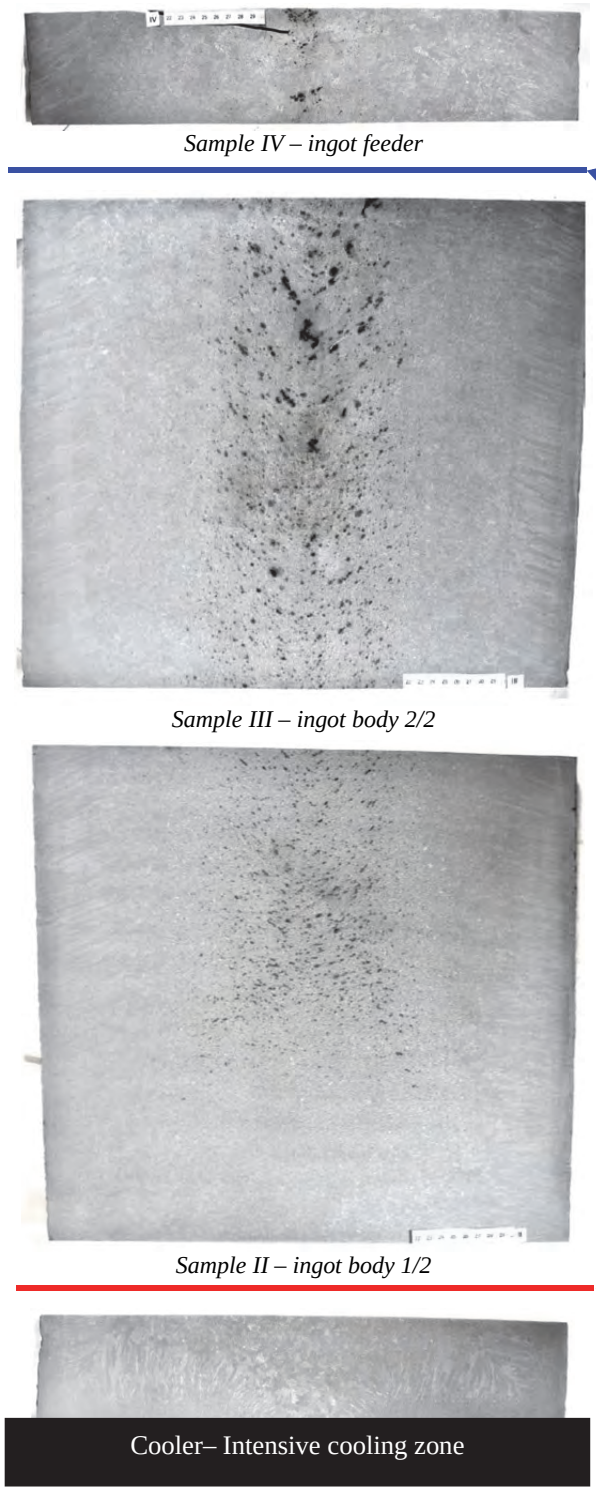

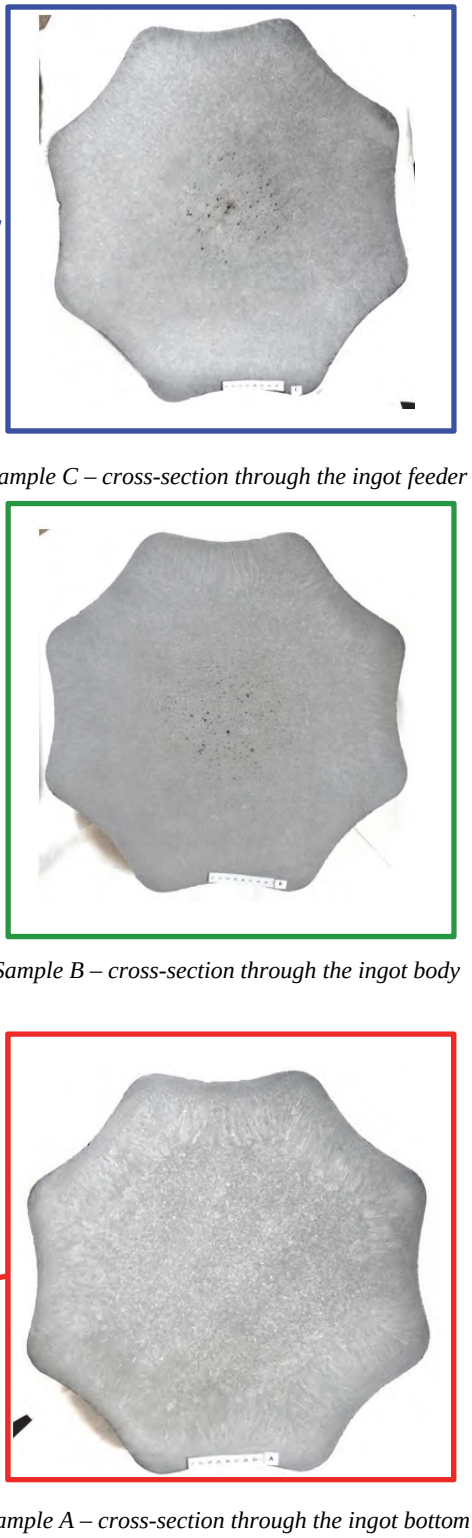

Fig. 2 Macrostructure in four zones of the axial longitudinal section through an ingot
Obr. 2 Makrostruktura ve čtyřech zónách osového podélného řezu ingotu

Fig. 3 The macrostructure in the cross sections of an ingot
Obr. 3 Makrostruktura v příčných řezech ingotu

Hutnické listy č. 3/2017, roč. LXX
ISSN 0018-8069

In the macrostructure of individual samples, the sizes of equiaxed and columnar crystals and grains in the central section, referred to as the zone of "coarse-grained" or equiaxed crystals, were measured. We also analysed areas with the highest porosity. The observed sizes of grains in each zone along the height of the ingot are shown in Tabs. 2 and 3.

Tab. 2 Analysis of the macrostructure in the ingot axis
Tab. 2 Analýza makrostruktury v ose ingotu

Sample	Equiaxed crystal thickness	Columnar crystal thickness [1)]	Porosity width in axis area
	(mm)		
IV – ingot feeder	0 to 5	55	60
III – ingot body 2/2	5	60	150
II – ingot body 1/2	5 to 15	75	180
I – ingot bottom	20	70[2)] / 110[3)] / 185[4)]	×××

Note: [1)] *measured in the direction away from the surface*
[2)] *measured vertically from the cooling pipe*
[3)] *measured vertically*
[4)] *measured horizontally*

Tab. 3 Analysis of the macrostructure in the cross-sections of an ingot
Tab. 3 Analýza makrostruktury v příčných řezech ingotu

Sample	Equiaxed crystal thickness	Columnar crystal thickness [1)]	Porosity width in axis area
	(mm)		
Cross-section C	5	60	130
Cross-section B	5	70	160
Cross-section A	15	75	0

Note: [1)] *measured in the direction away from the surface*

The evaluation of the macrostructure in Fig. 2 shows that there is a thin strip of surface equiaxed crystals in the ingot axis, which is located 20 to 5 mm deep from the bottom of an ingot to the ingot feeder. This strip continuously changes into a zone of highly regulated columnar crystals. The zone of columnar crystals is most significant in sample I (the ingot bottom). In this sample, the thickness of columnar crystals ranges from 70 to 185 mm, which can be justified by the intense cooling of the ingot mould during the crystallization and solidification process of the ingot. From the bottom toward the feeder of the ingot, thickness of this layer decreases in the range of 75 to 55 mm. Both above noted layers are followed by the area of coarse-grained and then of finer-grained equiaxed crystals found in the axial area of the ingot.

Fig. 2 shows the occurrence of numerous, mostly tiny cavities in the axial area stretching from the ingot feeder to a depth of approximately 765 mm, while the most significant porosity has been identified in a/the sample II (an ingot body 1/2). However, the tiny cavities in the axial area do not occur in sample I (an ingot bottom) and only partially occur in sample II (an ingot body 1/2) up to a height of about 335 mm, which is related to the effect on crystallization and solidification of the ingot due to intense cooling. The above-mentioned distribution of respective zones was also confirmed on transverse sections (Fig. 3).

When comparing the macrostructure of a non-cooled (Fig. 4) and cooled ingot (Fig. 5), the effect of intensive heat transfer is evident, especially on the shape of columnar crystals and the porosity, which starts 100 mm higher in the axial section in the case of the cooled ingot compared to the non-cooled one. The measured dimensions of respective zones along the height of both ingots are shown in Fig. 6 and 7. The main features of the macrostructure (porosity and the occurrence of columnar crystals) of the two ingots are compared in Fig. 8.

Fig. 4 Macrostructure in the ingot axis, Experiment Part 1
Obr. 4 Makrostruktura v ose ingotu, experiment část 1

Fig. 5 Macrostructure in the ingot axis, Experiment Part 2
Obr. 5 Makrostruktura v ose ingotu, experiment část 2

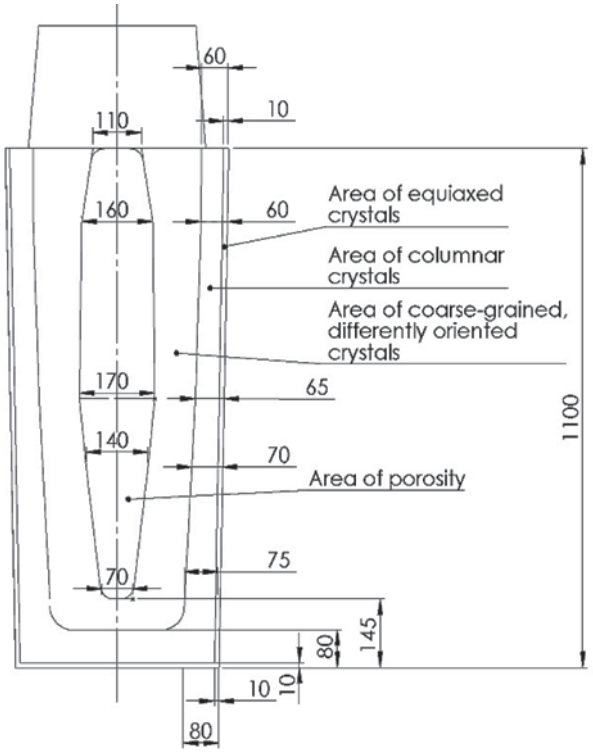

Fig. 6 Schematic analysis of macrostructure in the ingot axis; Experiment Part 1

Obr. 6 Schématická analýza makrostruktury v ose ingotu, experiment část 1

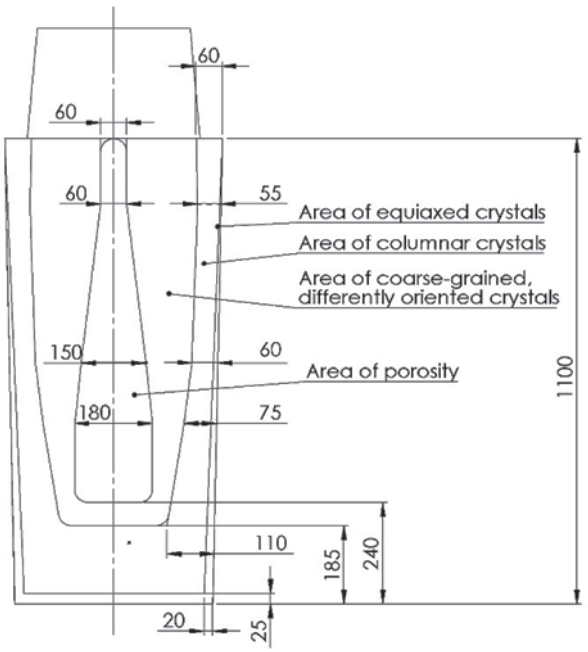

Fig. 7 Schematic analysis of macrostructure in the ingot axis; Experiment Part 2

Obr. 7 Schématická analýza makrostruktury v ose ingotu, experiment část 2

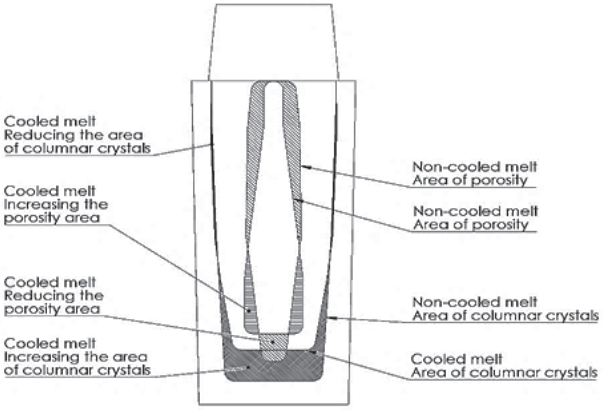

Fig. 8 Schematic analysis of macrostructure in the ingot axes; Experiment Part 1 and Part 2

Obr. 8 Schématická analýza makrostruktury v osách ingotů, experiment část 1 a 2

Macrostructure characteristics; Experiment Part 1:

The zone of equiaxed crystals (the edge of the ingot) extends to a depth of approx. 10 mm from the edge.

The zone of columnar crystals along the ingot height ranges from 75 mm (ingot bottom) to 60 mm (upper part of the ingot body). In the ingot axis, the columnar crystals extend 80 mm from the bottom into the ingot body.

In the centre of the ingot there is a zone of coarse-grained or equiaxed crystals with significant porosity, which is 110 mm wide in the upper part of the ingot, widens to 160-170 mm towards the centre and decreases in the bottom down to 70 mm.

Macrostructure characteristics; Experiment Part 2:

The zone of equiaxed crystals (the edge of the ingot) extends to a depth of 20 mm from the edge near the bottom, and along the height of the ingot decreases down to 0 mm under the topping.

The zone of columnar crystals along the ingot height ranges from 110 mm at the ingot bottom to 55 mm near the topping. In the ingot axis, the columnar crystals reach 185 mm from the bottom to the ingot's body.

In the centre of the ingot there is a zone of coarse-grained i.e. equiaxed crystals with significant porosity, which is 110 mm wide in the upper part of the ingot, expands to 160 - 170 mm towards the centre and decreases in the bottom down to 70 mm.

At the centre of the ingot, there is a zone of coarse-grained i.e. equiaxed crystals with significant porosity that is 60 mm wide at the top of the ingot, extends to 180 mm at the centre of the ingot and then abruptly tapers and no longer occurs at the bottom of the ingot.

Also, macrostructure analysis was performed in cross-sections A, B and C, which corresponded to the findings obtained from macrostructure analysis in longitudinal sections of the ingot axis.

Hutnické listy č. 3/2017, roč. LXX
ISSN 0018-8069

The assessment of the macrostructure of the floor of the ingots revealed that in both cases, the pores were closed due to solidification of the ingot body and the topping zone. This points to an inadequate function of the feeder to refill the ingot body with molten metal. This finding resulted in optimization of the shape and size of the ingot feeder.

2.2 Evaluation of chemical composition

To evaluate the chemical composition, the accredited test QI-ISO-LAB1-10-09 "Determination of Carbon and Sulphur Content" using the LECO CS 230 analyser and also the accredited test QI-ISO-LAB1-10-04 "RTG Spectrometry Practices" using the ARL ADVANT'X IntellipowerTM x-ray fluorescence spectrometer were used. To determine the ingot homogeneity, we only determined C, Cr and Mo contents.

Metal samples from the centre of the ingot to its edge were removed from cross-sections A, B and C. In the axis, the samples were marked No. 1 and then evenly removed all the way to the edge of the ingot. The process of change of the element content in the cross-section as well as the degrees of segregation is presented in Tab. 4, which describes the contents of elements both for the Experiment Part 1 and Part 2. For each element, the first column shows the non-cooled melt values (Experiment Part 1) and the second column shows the cooled melt values (Experiment Part 2). The graphical element contents in cross-sections of the ingot are shown in Fig. 9 for the carbon, in Fig. 10 for the chrome and in Fig. 11 for the molybdenum. In Figs. 9 – 11, the values for the Experiment Part 1 are highlighted with a solid blue line; the values for the Experiment Part 2 are highlighted with red.

Tab. 4 Chemical composition of the samples in cros-section A, B and C of the ingot - the first measurement
Tab. 4 Chemické složení vzorků odebraných po průřezu ingotu v řezech A, B a C – první měření

Sampling location	Designation	Element content (wt. %)						Segregation coefficient (1)					
		C splinters		Cr		Mo		C/Co		Cr/Cr		Mo/Mo	
		Non-cooled	Cooled	Non-cooled	Cooled	Non-cooled	Cooled	Non-cooled	Cooled	Non-cooled	Cooled	Non-cooled	Cooled
Ingot bottom	A1	0.95	1.01	1.52	1.54	1.25	1.30	0.95	1.00	0.99	0.99	1.01	1.03
	A2	0.98	1.01	1.52	1.54	1.27	1.29	0.98	1.00	0.99	0.99	1.02	1.02
	A3	0.99	1.01	1.53	1.54	1.28	1.29	0.99	1.00	1.00	0.99	1.03	1.02
	A4	1.03	1.02	1.54	1.55	1.28	1.30	1.03	1.01	1.01	1.00	1.03	1.03
	A5	1.03	1.03	1.55	1.56	1.30	1.31	1.03	1.02	1.01	1.01	1.05	1.04
Ingot body	B1	0.97	0.97	1.50	1.50	1.23	1.22	0.97	0.96	0.98	0.97	0.99	0.97
	B2	1.00	0.99	1.51	1.52	1.24	1.26	1.00	0.98	0.99	0.98	1.00	1.00
	B3	1.02	1.01	1.54	1.55	1.28	1.29	1.02	1.00	1.01	1.00	1.03	1.02
	B4	1.03	1.04	1.55	1.55	1.29	1.30	1.03	1.03	1.01	1.00	1.04	1.03
	B5	1.03	1.02	1.55	1.56	1.29	1.31	1.03	1.01	1.01	1.01	1.04	1.04
Under ingot topping	C1	1.01	1.01	1.51	1.54	1.22	1.30	1.01	1.00	0.99	0.99	0.98	1.03
	C2	1.01	1.03	1.52	1.55	1.26	1.32	1.01	1.02	0.99	1.00	1.02	1.05
	C3	1.02	1.04	1.55	1.56	1.30	1.33	1.02	1.03	1.01	1.01	1.05	1.06
	C4	1.01	1.04	1.55	1.56	1.28	1.31	1.01	1.03	1.01	1.01	1.03	1.04
	C5	0.99	1.01	1.55	1.56	1.29	1.31	0.99	1.00	1.01	1.01	1.04	1.04
Melt in CL		1.00	1.01	1.53	1.55	1.24	1.26	-	-	-	-	-	-

2.2.1 Evaluation of chemical composition, Experimental Part 1

Tab. 4 and Figs. 9 – 11 show that the element contents tend to be decreasing in the axis part of the ingot, and vice versa, towards the edge of the ingot are increasing. They also show that C and Cr have a negative segregation at the bottom in the ingot axis, which changes into a positive one toward the edge of the ingot. A similar trend, though smaller, applies to C and Cr in the body of the ingot. Under the ingot feeder, Cr in the axial part of the ingot has a negative segregation, which toward the edge changes into a positive one. In contrast, C shows a predominantly positive segregation across the entire cross-section under the feeder. Mo has a positive segregation at the bottom of the ingot across the entire cross-section. In contrast, in the body of the ingot and under the feeder of the ingot, Mo shows a negative segregation in the axial part, which changes into the positive toward the edge.

2.2.2 Evaluation of chemical composition, Experimental Part 2

Tab. 4 and Figs. 9 – 11 show that the C, Cr and Mo element contents are lower in the ingot body (section B) and in the ingot bottom (section A), and their content increases toward the ingot edge. The same trend of increase in the content of elements from the centre

toward the edge of the ingot is also apparent in the section below the ingot topping. In terms of segregation, there is a positive C and Mo segregation across the entire cross-section, both at the bottom of the ingot as well as in the section under the topping and the negative segregation in case of Cr in the central part, which transitions in a positive segregation in the edge part of the ingot. In a central section of the body of the ingot, there is a negative segregation of C, Cr and Mo that switches toward the edge of the ingot in the positive one. The figures show that the greatest differences in the element contents in the body of the ingot can be found between the central and the edge part of the ingot, with this applying for C and Cr, as well as for Mo.

2.2.3 Comparison of results of the chemical composition of Experiment Part 1 and Experiment Part 2

Comparison of the non-cooled and cooled ingot shows that the evaluated C, Cr and Mo elements at the bottom have very little negative segregation due to the intense heat transfer from the melt when the ingot is solidified. A smaller difference in segregation has been observed in the centre along the ingot height. On the contrary, in the section under the topping, the segregation of C and, in particular, of Cr and Mo is lower for the cooled ingot than for the non-cooled.

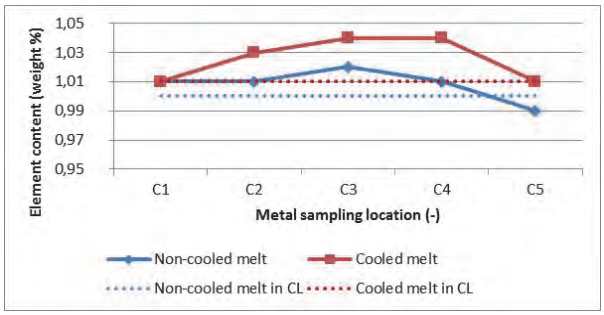

a) Section C - under the ingot feeder
a) řez C – pod hlavou ingotu

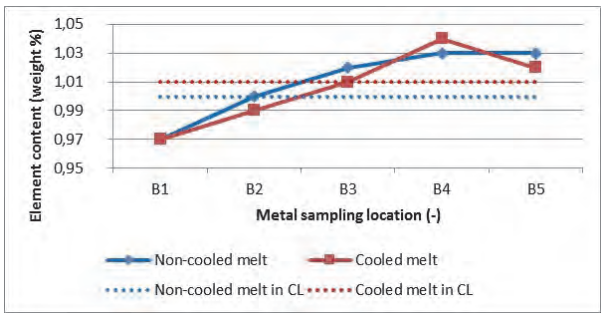

b) Section B – ingot body
b) řez B – tělo ingotu

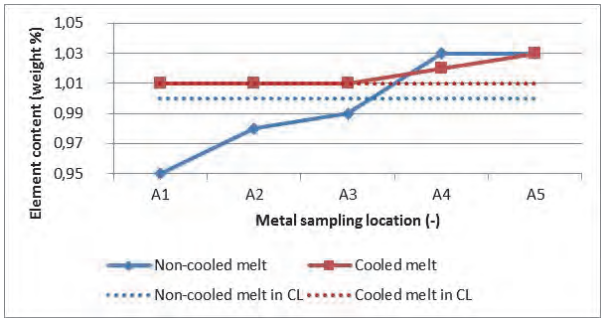

c) Section A – bottom part of ingot
c) řez A – pata ingotu

Fig. 9 Course of the content of carbon in cross-sections of the ingot (A-bottom, B-body, C-under the topping)

Obr. 9 Průběh obsahu uhlíku v příčných řezech ingotu, A-pata, B-tělo, C-pod hlavovým nástavcem

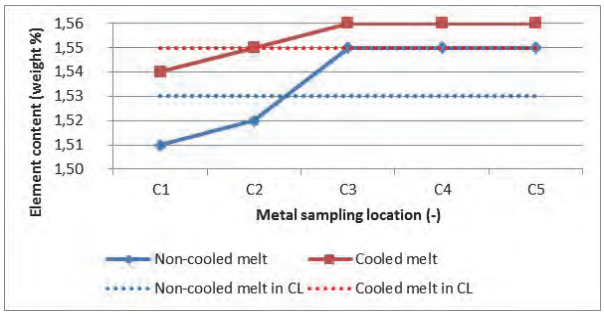

a) Section C - under the ingot feeder
a) řez C – pod hlavou ingotu

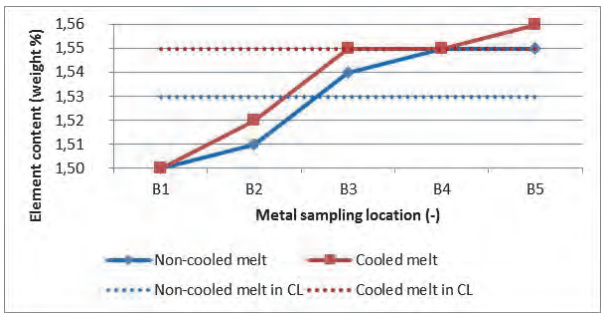

b) Section B – ingot body
b) řez B – tělo ingotu

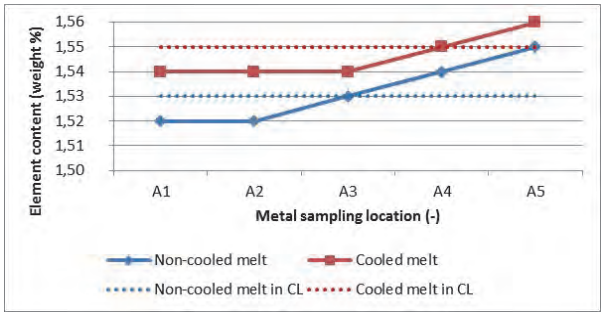

c) Section A – bottom part of ingot
c) řez A – pata ingotu

Fig. 10 Course of the content of chromium in cross-sections of the ingot (A-bottom, B-body, C-under the topping)

Obr. 10 Průběh obsahu chromu v příčných řezech ingotu, A-pata, B-tělo, C-pod hlavovým nástavcem

Hutnické listy č. 3/2017, roč. LXX
ISSN 0018-8069

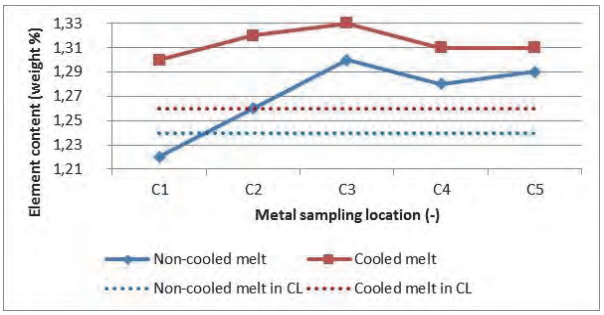

a) Section C – under the ingot feeder
a) řez C – pod hlavou ingotu

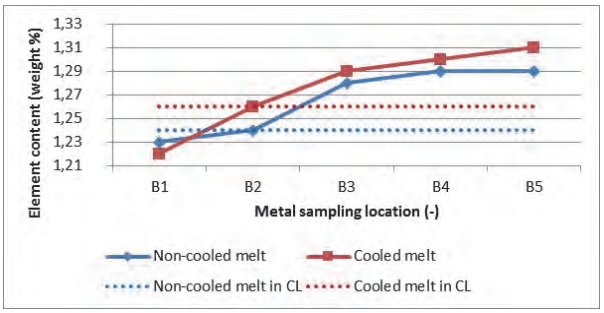

b) Section B – the ingot body
b) řez B – tělo ingotu

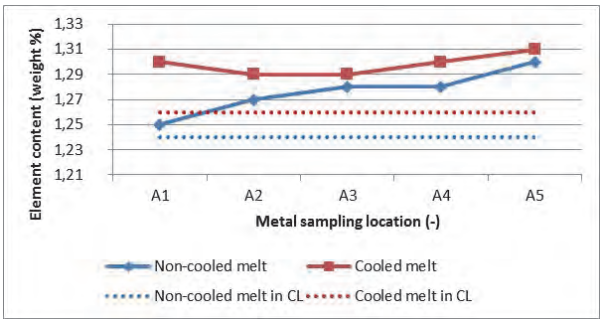

c) Section A – bottom part of the ingot
c) řez A – pata ingotu

Fig. 11 Course of the content of molybdenum in cross-sections of the ingot (A-bottom, B-body, C-under the topping)
Obr. 11 Průběh obsahu molybdenu v příčných řezech ingotu, A-pata, B-tělo, a C-pod hlavovým nástavcem

2.3 Evaluation of the thermal score of an ingot mould

For both parts of the experiment, i.e. in the case of non-cooled and cooled ingots, the thermal score of the mould-ingot system was determined. The heat transferred from the mould surface, the heat accumulated in a mould wall and feeder was determined; the heat transferred by the cooling medium was calculated, and finally the enthalpy of the ingot was determined.

To obtain the conditions necessary to determine the heat score items, the ingot mould was equipped with sensors and measuring apparatus that recorded the measured quantities with a period of one second. The jacketed thermocouples were placed in the wall of the mould as shown in Fig. 12. At three vertical levels, pairs of thermocouples were installed; each time with one measuring joint placed in a borehole at a distance of 5 mm from the inner surface of the mould and with the other mechanically fixed on the outer surface. The first index indicating the measured temperatures in the Figure means the order of a vertical level of the sensors, starting from the casting plate, the second "i" index indicates the sensor at the inner surface, the "e" index indicates the sensor on the outer surface.

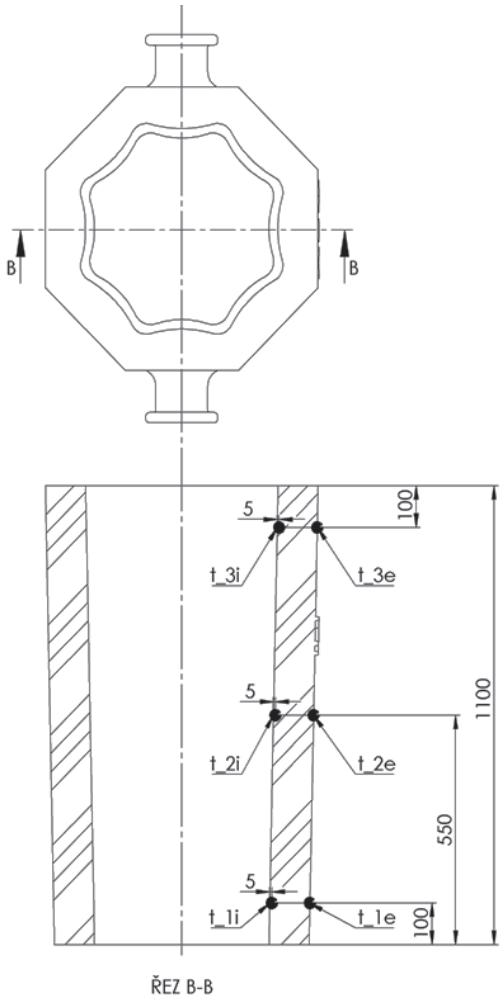

Fig. 12 Placement of thermocouples in the wall of the mould
Obr. 12 Umístění termočlánků ve stěně kokily

The progress of temperatures measured in the ingot mould wall are in the case of non-cooled ingot plotted graphically in Fig. 13; the measured temperatures in the case of cooled ingot are shown in Fig. 14. The similarity of temperature curves at the horizontal levels no. 2 and no. 3 and simultaneously, the dissimilarity of curves at level no. 1 (especially the dissimilarity of t_1i curves) shows that the influence of additional cooling is significant especially in the lower part of an ingot mould, or an ingot itself.

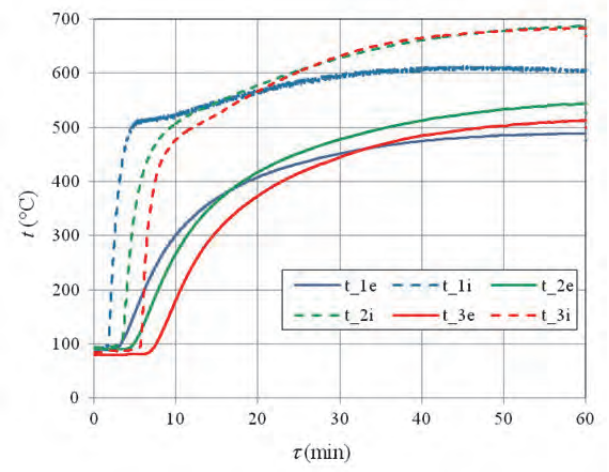

Fig. 13 Temperatures measured in the wall of non-cooled mould
Obr. 13 Teploty měřené ve stěně nechlazené kokily

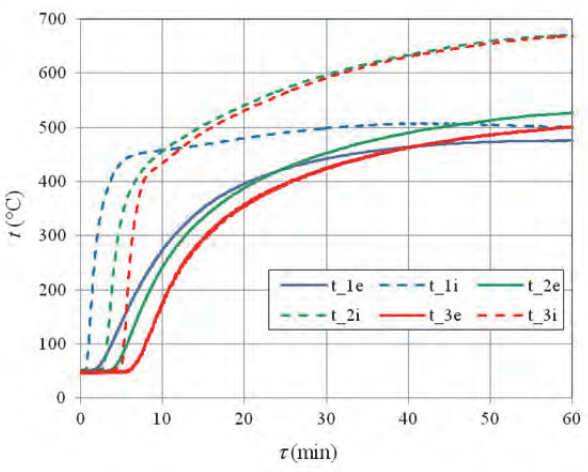

Fig. 14 Temperatures measured in the wall of cooled mould
Obr. 14 Teploty měřené ve stěně chlazené kokily

In the case of a cooled mould, the flow rate and temperatures of the cooling media, i.e. air and water, were measured. Air-cooling took 30 seconds, after that cooling water was applied. Flow rates were determined by volume method and re-calculated to mass flows of 0.34 kg·s^{-1} of air and 0.94 kg·s^{-1}of water. Temperatures of the cooling media were measured by sensors located on the outer surface of the inlet and outlet piping. The pipe sections near the sensors were thermally insulated against their surroundings. The measured values were corrected to eliminate the influence of the heat capacity of the pipe wall and the transport delay of the medium.

The heat score of ingot can be written in the following equation:

$$\Delta H_{\text{steel}} = Q_{\text{cool}} + Q_{\text{amb}} + Q_{\text{acc}} + Q_{\text{oth}} \quad \text{(J)} \qquad (1)$$

where ΔH_{steel} (J) is the heat loss of the enthalpy of the steel, Q_{cool} (J) is the heat transferred by the cooling medium, Q_{amb} (J) is the heat transferred to the surrounding by the convection and the radiation, Q_{acc} (J) is the heat accumulated in the wall of the mould and in the feeder, and Q_{oth} (J) are other less important heat items that have been neglected in the calculation, such as accumulated heat in ingot hinges, heat removed from the steel in the inlet system, heat transferred by leading it to the casting plate.

The heat transferred by the cooling medium was determined by continuous integration of the heat flow P_{cool} from the beginning of the filling of the mould. The heat flowing to the cooling medium was calculated as follows:

$$P_{\text{cool}} = Q_{\text{m}} \cdot (h_{\text{out}} - h_{\text{in}}) \quad \text{(W)} \qquad (2)$$

where Q_{m} (kg·s^{-1}) is the mass flow of the cooling medium, h_{in} and h_{out} (J·kg^{-1}) are the specific enthalpy of the cooling medium at the inlet and outlet of the cooler at temperatures of the cooling medium t_{in} and t_{out} (°C). The specific enthalpies were calculated using the temperature-dependent regression functions according to physical tables [2].

The heat transferred to the surroundings through the ingot mould wall could be determined in the case of stationary process from the density of heat flow in the wall using temperatures measured by thermocouples in the wall. In the given case, however, it was a non-stationary process with significant heat accumulation in the mould wall, and therefore this method could not be used. Heat transferred to the surroundings was calculated from the measured surface temperatures of the mould using physical laws of free convection and radiation. The zonal method was used in the calculations, where the mould was divided into three sections along its height, and the fourth section was formed by a topping.

In each measured moment, values of the Grashof and Prandtl criteria were determined and the Nusselt criterion and subsequently the heat transfer coefficient and the convection heat flow [3] were calculated using the free convection curve equation. The heat flow through radiation was calculated using the theory of radiation between the body and the surrounding surfaces for the emissivity of the mould surface 0.8 and the ambient temperature of 20 °C. The heat transferred from the surface of the mould into the surroundings was then obtained by integrating the total heat flow through convection and radiation from the start of casting.

The heat accumulated in the mould wall and in the topping was calculated from the increase of enthalpy in the mould with a topping from the start of casting up to current time:

$$Q_{\text{acc}} = m_{\text{m}} \cdot (h_{\text{m}} - h_{\text{m,0}}) \quad \text{(J)} \qquad (3)$$

where m_{m} (kg) is the weight of an ingot mould with a feeder, h_{m} and $h_{\text{m,0}}$ (J·kg^{-1}) are the specific enthalpies

Hutnické listy č. 3/2017, roč. LXX
ISSN 0018-8069

of the ingot mould with the feeder at that moment and at the start of casting determined for the average mould wall temperatures at that moment t_m (°C) and at the beginning of casting $t_{m,0}$ (°C). Average wall temperatures in individual mould sections and in the feeder were interpolated from the measured temperatures both along the mould height and in the radial direction using the theoretical temperature profile in the wall, which was replaced by a cylindrical wall of equivalent cross-section for this purpose. Thermo-physical parameters of cast steel and ingot (specific enthalpy, density) were determined using temperature-dependent CompuTherm software.

In the charts shown in Figs. 15 and 16, the heights of each colour-coded area in each moment represent the heat accumulated in the wall of the mould Q_{acc} (J), the heat transferred to the surroundings Q_{amb} (J), and the heat transferred through a cooling medium Q_{cool} (J), as a function of time. The total height of all areas approximately represents the loss of the ingot's enthalpy while neglecting the heat of other Q_{oth} heat items.

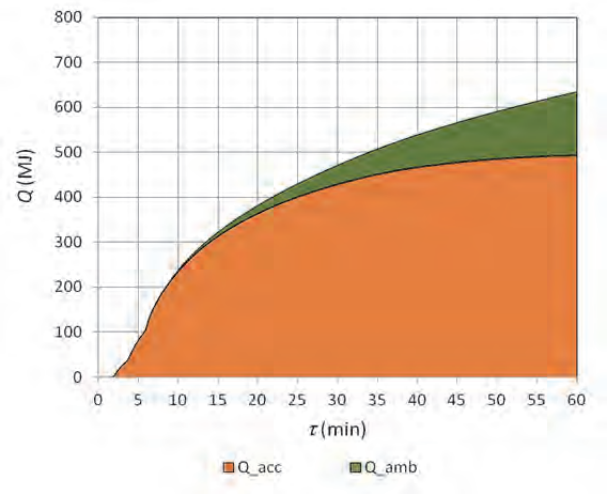

Fig. 15 Items of thermal score of non-cooled ingot
Obr. 15 Položky tepelné bilance nechlazeného ingotu

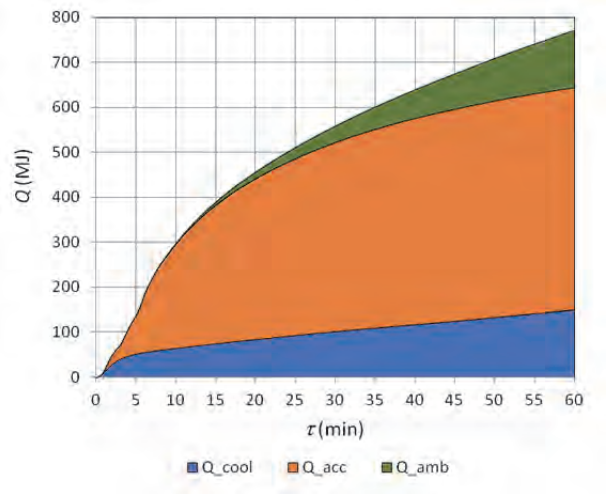

Fig. 16 Items of thermal score of cooled ingot
Obr. 16 Položky tepelné bilance chlazeného ingotu

The time progress of individual heat score items according to equation (1) and the total enthalpy ingot curve (marked as *H_steel*) are shown in Fig. 17 for a non-cooled ingot, and Fig. 18 for a cooled ingot.

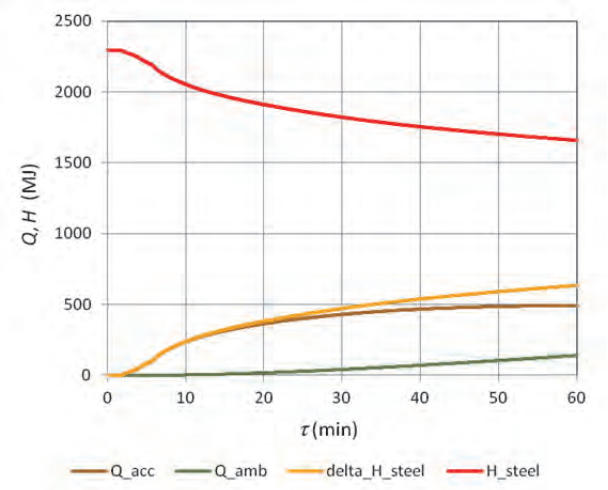

Fig. 17 Items of thermal score of non-cooled ingot and enthalpy of ingot
Obr. 17 Položky tepelné bilance nechlazeného ingotu a entalpie ingotu

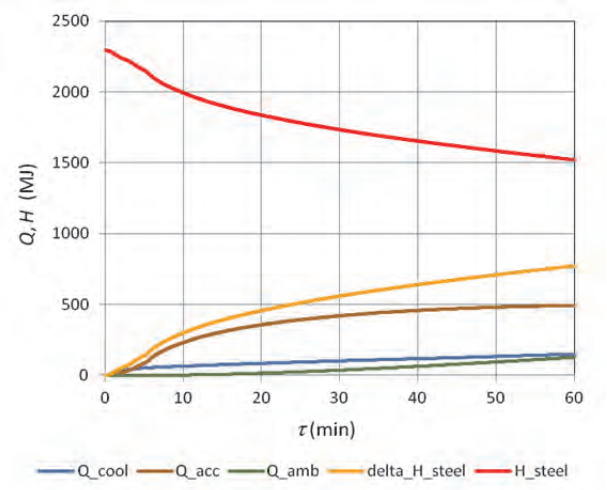

Fig. 18 Items of thermal score of cooled ingot and enthalpy of ingot
Obr. 18 Položky tepelné bilance chlazeného ingotu a entalpie ingotu

The final values of the heat score items after 60 minutes from the start of casting, supplemented with ingot enthalpy items, specific enthalpy and mean ingot temperatures are summarized in Tab. 5. Average temperature, or specific enthalpy of the ingot corresponds to the average proportion of the solid phase f_s for the entire ingot. Since the ingot temperature is not homogeneous, the value 100 % does not necessarily mean that the steel is solid throughout the entire ingot volume.

Tab. 5 Items of thermal score of a cooled mould, and enthalpy and temperature in an ingot after 60 min. of solidification
Tab. 5 Položky tepelné bilance chlazené kokily, entalpie a teplota ingotu po 60 min. tuhnutí

Quantity	Designation	Non-cooled ingot	Cooled ingot
Heat removed by cooling	Q_{cool} (MJ)	0	151
Heat accumulated in mould	Q_{acc} (MJ)	494	493
Heat transferred to surroundings	Q_{amb} (MJ)	141	128
Loss of enthalpy of ingot	ΔH_{steel} (MJ)	635	772
Resulting enthalpy of ingot	H_{steel} (MJ)	1658	1521
Resulting specific enthalpy of ingot	h_{oc} (kJ·kg^{-1})	981	900
Resulting average temperature of ingot	t_{steel} (°C)	1342	1243
Resulting average proportion of solid phase	f_s (%)	86	100

Comparison of the heat scores of both the non-cooled and the cooled ingot means that approx. 20% more heat was transferred from the cooled ingot than from the non-cooled ingot within the same period of time, i.e. 772 MJ from the cooled ingot versus 635 MJ from the non-cooled ingot.

The heat accumulated in a mould wall and in a feeder was approximately of the same size in both cases, making up for the largest amount of heat transferred from the solidifying steel; for a non-cooled ingot it was 78 % (i.e. 494 MJ from a total of 635 MJ), for a cooled ingot it was 64 % (i.e. 493 MJ from a total of 772 MJ). The heat transferred to the surroundings from the surface of the mould by convection and radiation amounted to 22 % of the heat transferred from the steel in the case of non-cooled ingot (i.e. 141 MJ from a total of 635 MJ) and 16 % in the case of cooled ingot (i.e. 128 MJ from a total of 772 MJ).

The heat transferred to the cooling medium from the cooled ingot represented approximately 20 % from the heat removed the ingot, i.e. 151 MJ from a total of 772 MJ. This was due to a direct contact of the cooler with the solidifying steel. The thermal resistance in the ingot material increases linearly with the distance through which the heat is transported to the cooler, therefore additional cooling predominantly affects the bottom part of the ingot, as also visible from the progress of temperatures measured in the wall of the mould.

Conclusions

The macro-structural characteristics and the analysis of chemical heterogeneity of a 14209Mo steel ingot cast into a V2A mould set as well as the calculations of the thermal scores were carried out.

The evaluation results of macrostructure in ingot sections show that the effect of intensive cooling of the cast ingot manifested itself greatly in the bottom of the ingot, where the zone of columnar crystals increased. The evaluation of the macrostructure also shows that in the cooled ingot compared to the non-cooled one, a porous area was increased in the ingot's lower part while this area in the ingot's upper part was significantly reduced. This may be due to an insufficient feeder function due to the intense cooling of the lower part of ingot.

Comparison of the chemical composition in ingot sections along its height and cross-section shows that the intense heat removal during casting and solidification of the ingot has a major effect on reducing the segregation of C, Cr and Mo elements.

Comparison of the calculated heat scores showed that in a given period of time approximately 20% of more heat was removed from a cooled ingot than from a non-cooled ingot. The highest increase in heat removal was detected at the bottom of the ingot.

The developed technology is protected by Czech patent No. 306 775.

Acknowledgements

The paper was completed within the framework of the project "Support of Science and Research in the Moravian-Silesian Region 2015."

Literature

[1] PINDOR, J., KURKA, V., ŠTEFANIŠINOVÁ, Š., SOCHA, L. Makrostruktura a chemická homogenita ocelového ingotu. *Hutnické listy*, 69 (2016) 4, 20–27. ISSN 0018-8069.

[2] BÁLEK, S. *Tepelně technické tabulky a diagramy*, 2. vyd. Ostrava: VŠB-TU Ostrava, 2005. ISBN 80-248-0828-5.

[3] PŘÍHODA, M., RÉDR, M. *Sdílení tepla a proudění*, 2. vyd. Ostrava: VŠB-TU Ostrava, 2008. ISBN 978-80-248-1748-4.

Na míru střižené bramy

Westdeutsche Allgemeine *14.03.2017*

Nabízet více než ocel je cílem Thyssen-Krupp Steel. Nabídka ocelářského koncernu je dnes rozšířena o další službu, umožněnou novou adjustáží, která byla uvedena do provozu v Beeckerwerthu. Mohou tam být zpracovávány bramy podle individuálních přání zákazníků. Bramy mohou být přiřezávány přesně podle přání zákazníka na šesti tzv. „stolech", autorem i stavitelem tohoto zařízení je Thyssen-Krupp Mill Services & Systems. V budoucnu zde má být zpracováváno až 150 000 tun bram.